ELSEVIER

Journal of Photochemistry and Photobiology A: Chemistry 91 (1995) 73–79

Journal of PHOTOCHEMISTRY AND PHOTOBIOLOGY A: CHEMISTRY

Photochemistry and photoinitiator properties of 2-substituted anthraquinones
1. Absorption and luminescence characteristics

Norman S. Allen [a], Graeme Pullen [a], Milla Shah [a], Michele Edge [a], Diane Holdsworth [a], Iain Weddell [b], Ron Swart [b], Fernando Catalina [c]

[a] *Chemistry Department, Faculty of Science and Engineering, Manchester Metropolitan University, Chester Street, Manchester M1 5GD, UK*
[b] *Zeneca Specialities Ltd., Blackely, Manchester M9 3DA, UK*
[c] *Instituto de Ciencia y Tecnologia de Polymeros, CSIC, 3 Juan de la Cierva, 28006 Madrid, Spain*

Received 4 April 1995; accepted 18 May 1995

Abstract

The photophysical and photochemical properties of 15 2-substituted anthraquinones were determined in various solvents. The absorption spectra revealed the presence of two types of structure: (1) a structure with a long-wavelength band around 360 nm associated with the electron-donating effects of the substituent; (2) a structure with a long- wavelength band around 320 nm associated with the electron-withdrawing effects of the substituent. Fluorescence and phosphorescence analyses indicate a high rate of intersystem crossing to the triplet state, with the relative positions of the lowest excited singlet $\pi\pi^*$ and second excited triplet $n\pi^*$ states playing an important role in determining the luminescence behaviour and subsequent photoactivity. The electron-withdrawing and electron-donating abilities of the 2-substituent are important in this regard. Two of the anthraquinones, 2-(4-phenyl)thiazoleanthraquinone and 2-chloroamidoanthraquinone, give anomalous dual phosphorescence emissions from both the triplet $\pi\pi^*$ and $n\pi^*$ states depending on the wavelength of excitation. The data are discussed in relation to the expected photoinitiation activities of the compounds.

Keywords: Photoinitiators; Anthraquinones; Absorption; Luminescence

1. Introduction

The photochemistry of anthraquinones, particularly dyes, has been investigated in some depth [1–5]. Much of the work has been related to their ability to photosensitize the degradation and oxidation of polymer systems, an effect often termed "phototendering" [4,5]. Other studies have concentrated on their photochemical stability as dyes [4,5]. Thus, whilst 2-substituted anthraquinone dyes, such as the 2-piperidino derivative, are light fugitive and known to phototender polymers such as nylon 6,6,1-substituted analogues are more light stable and photoprotect the polymer [3–5]. The photoreaction mechanisms of anthraquinones are controversial and, to date, are still unresolved. Two mechanisms have been invoked to account for the activity of anthraquinones. These include a photoreduction process, involving electron or hydrogen atom abstraction from the polymer by the anthraquinone chromophore, or the sensitization of singlet oxygen by the quenching of the photoexcited triplet state of the anthraquinone by ground state molecular oxygen [5]. The mechanisms are further complicated by the nature of the polymer and the environment. As far as photoinduced polymerization is concerned, the former mechanism appears to be the only likely contender to account for the high efficiency of the reactions since the role of singlet oxygen is not important.

Our previous work [6–8] on the photoinduced crosslinking properties of 2-acrylamidoanthraquinone and 2-acryloxyanthraquinone molecules showed the former to exhibit a high degree of activity. This was associated with the importance of a long-lived, active, low-lying, excited triplet state. The less active 2-acryloxyanthraquinone was observed to give rise to emission from its upper excited triplet $n\pi^*$ state [9]. In this work, we have undertaken a more detailed solution spectroscopic and photopolymerization study on a wide range of novel 2-substituted anthraquinones (structures 1–15).

1010-6030/95/$09.50
SSDI 1010-6030(95)04120-6

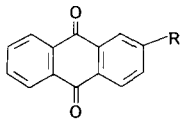

1. R = Br
2. R = -$CHBr_2$
3. R = -CCl_3
4. R = 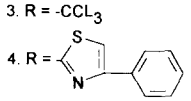
5. R = -NH-C(O)- 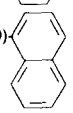
6. R = -NH-C(O)CL
7. R = -NH-C(O)-$CH(CH_2CH_3)(CH_2CH_2CH_2CH_3)$
8. R = -NH-C(O)-$(CH_2)_7CH{=}CH(CH_2)_7CH_3$
9. R = -NH-C(O)-O-CH_2CH_3
10. R = -$N(C(O)\text{-}CH_3)(CH_2CH(CH_3)_2)$
11. R = -$N(C(O)\text{-}CH_3)((CH_2)_5CH_3)$
12. R = -$C(O)OCH_3$
13. R = -C(O)- 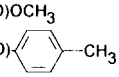 -CH_3
14. R = -C(O)-NH- 
15. R = -O-C(O)-$N(C_2H_5)_2$

This comparative study enables the importance of structural features to be interrelated to the photophysical and photoinduced polymerization properties. We reveal a number of unique features associated with the photophysical properties of the anthraquinones which explain their unusual photochemical behaviour.

2. Experimental details

2.1. Materials

The compounds 2-bromoanthraquinone (**1**) (melting point (m.p.) = 209 °C), 2-(1,1-dibromomethyl)anthraquinone (**2**) (m.p. = 225 °C), 2-(1,1,1-trichloromethyl)anthraquinone (**3**) (m.p. = 154.5 °C), 2-(4-phenyl)thiazoleanthraquinone (**4**) (m.p. = 204.5 °C), 2-chloroamidoanthraquinone (**6**) (m.p. = 283(d) °C), 2-(2-ethyl)hexylamidoanthraquinone (**7**) (m.p. = 141.5 °C), 2-(octadecyl-8-ene)amidoanthraquinone (**8**) (m.p. = 125.5 °C), 2-ethoxyamidoanthraquinone (**9**) (m.p. = 265(d) °C), 2-(*N*-2-methylpropyl)methylamidoanthraquinone (**10**) (m.p. = 180.5 °C), 2-(*N*-*n*-hexyl)methylamidoanthraquinone (**11**) (m.p. = 57 °C), 2-methylcarboxyanthraquinone (**12**) (m.p. = 163 °C), 2-(4-methyl)benzoylanthraquinone (**13**) (m.p. = 179 °C), 2-(*N*-phenyl)carboxamidoanthraquinone (**14**) (m.p. = 334(d) °C) and 2-(*N*,*N*-diethyl)-amidooxyanthraquinone (**15**) (m.p. = 104 °C) were supplied by the Fine Chemicals Service of Zeneca Specialities, Blackely, Manchester, UK. All the solvents used in this work were obtained from Aldrich Chemical Co. Ltd., UK and were of spectroscopic or high performance liquid chromatography (HPLC) grade quality. The compound 2-naphthylamidoanthraquinone (**5**) (m.p. = 229–231(d) °C) was prepared as described below.

2-Aminoanthraquinone (2.23 g; 0.01 mol) was dissolved in tetrahydrofuran (THF) (60 cm^3) together with 1-naphthoyl chloride (1.65 cm^3; 2.106 g; 0.011 mol) and triethylamine (1.0 cm^3). The reaction mixture was stirred for 48 h at room temperature. Thin layer chromatography (TLC) analysis revealed a product with an R_f value of 0.42 in an ethyl acetate–hexane mixture (1 : 1). The product was isolated by column chromatography using silica. A yellow product was obtained in low yield (0.124 g; 3.3%) with a melting point of 229–231 °C. Mass spectral analysis gave a molecular ion peak at 377 *m/e* consistent with structure **5**. ^1H Fourier transform nuclear magnetic resonance (FT NMR) analysis confirmed several complex peaks in the region 7.5–9.0 ppm due to both the naphthyl and anthraquinone protons. ^{13}C FT NMR was more conclusive with a doublet due to the anthraquinone carbonyls at 181/183 ppm, an amide carbonyl singlet at 168 ppm and separate aromatic carbon atoms adjacent to the amide carbonyl at 145 ppm and amide nitrogen at 117 ppm. FTIR analysis confirmed the presence of the amide group at 1640 cm^{-1}.

2.2. Spectroscopic measurements

Absorption spectra were obtained using a Perkin–Elmer oLambda 7 absorption spectrometer. Fluorescence and phosphorescence excitation and emission spectra were obtained using a Perkin–Elmer LS-50B research luminescence spectrometer. Fluorescence quantum yields were obtained by the relative method using quinine sulphate in 0.1 M sulphuric acid as standard [10]. The quantum yield of quinine sulphate was assumed to be 0.55. Phosphorescence quantum yields were obtained in ethanol at 77 K using the relative method with benzophenone as a standard assuming a quantum yield of 0.74 in ethanol [11]. All spectra were corrected using a Perkin–Elmer IBM compatible GEM package with an appropriate file for this purpose.

3. Results and discussion

3.1. Absorption spectra

The absorption spectra of all 15 compounds were obtained in a series of solvents (chloroform, ethanol, acetonitrile and dimethylformamide) with increasing dielectric constant [12]. Solvents of lower polarity were unsuitable in terms of the solubility of most of the compounds. The spectroscopic properties of anthraquinones are well documented [4,5,13]. Normally, substitution in the 1-position gives rise to a stronger auxochromic effect, and hence a greater bathochromic shift, than an equivalent substitution in the 2-position. This is associated with strong charge transfer interaction with the ring system via the adjacent quinone group which can often take the form of intramolecular hydrogen bonding. This effect is not normally observed with 2-substituted anthraqui-

Table 1
Absorption data for 2-substituted anthraquinones

Anthraquinone	Chloroform		Ethanol		Acetonitrile		Dimethylformamide	
	λ_{max} (nm)	log ϵ	λ_{max} (nm)	log ϵ	λ_{max} (nm)	log ϵ	λ_{max} (nm)	log ϵ
1	331	3.77	329	3.78	327	3.88	329	3.89
2	330	3.79	328	3.79	327	3.76	329	3.80
3	328	3.68	325	3.83	323	3.70	326	3.86
4	392	3.87	387	3.82	383	3.90	388	3.94
5	370	3.67	368	3.69	368	3.86	376	3.58
6	419	3.61	448	3.76	426	3.67	438	3.82
7	369	3.63	369	3.84	371	3.67	376	3.74
8	366	3.54	366	3.66	371	3.43	379	3.58
9	372	3.55	377	3.84	372	3.61	381	3.64
10	334	3.61	328	3.79	328	3.66	330	3.72
11	357	3.37	328	3.76	329	3.82	330	3.69
12	330	3.66	326	3.79	323	3.55	328	3.82
13	328	4.01	326	3.85	325	3.74	328	3.85
14	332	3.84	329	4.16	328	3.75	332	3.80
15	330	3.75	326	3.73	326	3.57	328	3.89

nones and consequently these molecules tend to be more photochemically reactive.

The data pertaining to the 2-substituted anthraquinones described here are novel, with the exception of those for the 2-bromo derivative. The longest wavelength absorption maxima for the compounds are important in terms of their photochemical activity, and these are shown in Table 1 together with their extinction coefficients. The derivatives **1–3** and **10–15** all possess a longest wavelength absorption maximum at approximately 330 nm which exhibits a small hypsochromic shift. This band, which is also present in anthraquinone, is associated with an $n\pi^*$ transition. All these groups are expected to exhibit an electron-withdrawing effect on the anthraquinone ring and therefore the degree of charge transfer interaction will be negligible. The spectrum for compound **11** is anomalous in chloroform in that it exhibits a long-wavelength weak charge transfer band at 357 nm. This effect was not observed in other solvents and is therefore assumed to be associated with complexation with the solvent. However, on the basis of their structures, both derivatives **10** and **11** would be expected to exhibit a strong $-I$ effect with the ring system. There may well be intramolecular hydrogen bonding within the substituent involving the amide carbonyl and the alkyl methylenes. This was confirmed by molecular modelling of the structures. Compounds **4–9**, on the other hand, exhibit a longest wavelength absorption maximum at approximately 360 nm which tends to undergo a bathochromic shift in solvents of increasing dielectric constant. However, the shift is variable and relatively small, indicative of strong mixing with a close lying $n\pi^*$ state.

3.2. Fluorescence spectra

The fluorescence emission maxima and quantum yields in all four solvents are shown in Table 2. It is interesting to note that, apart from the anomalously high values for derivatives **4** and **6** in chloroform, both exhibit very low quantum yields. However, the computer enhancement facility of the LS-50B luminescence spectrometer allows the spectra to be measured. This suggests a high rate of internal conversion to the ground state or intersystem crossing to the triplet state. Consistent with the absorption data, derivatives **1–3** and **10–15** exhibit weak fluorescence that tends to undergo a hypsochromic shift in solvents of increasing dielectric constant. This effect is particularly notable in dimethylformamide and is associated with the $n\pi^*$ configuration of the lowest excited singlet state. In the case of derivatives **4–9**, there is a tendency for the emission maxima to shift to the red consistent with the $\pi\pi^*$ configuration of the lowest lying singlet.

The anomalous higher fluorescence quantum yields of derivatives **4** and **6** in chloroform may be associated with the effect of solvent polarity and structure on the energy levels as will be discussed later. Anomalous fluorescence emissions were also observed from the 2-naphthylamido derivative. These are illustrated in Fig. 1 for chloroform. Two different spectra, although very weak ($\phi_f < 10^{-5}$), were observed on excitation with wavelengths of less than 320 nm and above 370 nm. These may be associated with emissions from two closely spaced singlet states as will be described below. The other likely possibility is the observation of emissions due to the separate naphthalene and anthraquinone moieties. Efforts to purify the derivative, i.e. by column chromatography, did not eliminate the phenomenon.

3.3. Phosphorescence spectra

The phosphorescence emission data, quantum yields and triplet lifetimes for all the derivatives are shown in Table 3. The derivatives may be divided into three types depending on the characteristic emissions and lifetimes. The first group containing the three halogenated derivatives **1–3** exhibits strong phosphorescence emission with a short lifetime of

Table 2
Fluorescence data for 2-substituted anthraquinones

Anthraquinone	Chloroform		Ethanol		Acetonitrile		Dimethylformamide	
	λ_{max} (nm)	ϕ_f	λ_{max} (nm)	ϕ_f	λ_{max} (nm)	ϕ_f	λ_{max} (nm)	ϕ_f
1	450, 529(s)	2.9×10^{-4}	–	–	460, 493, 540(s)	1.4×10^{-4}	439, 578(s)	6.2×10^{-5}
2	405(s), 447	9.4×10^{-4}	–	–	445	$<10^{-5}$	440	1.3×10^{-4}
3	406(s), 446	7.6×10^{-4}	–	–	447, 599	$<10^{-5}$	432, 447	2.1×10^{-4}
4	540(s), 553	0.045	404, 549	1.2×10^{-4}	453(s), 505	4.8×10^{-4}	450, 599	3.7×10^{-4}
5	416	$<10^{-5}$	400	1.2×10^{-3}	405(s), 450, 478(s)	1.0×10^{-4}	427(s), 490(s), 497	2.7×10^{-4}
6	525, 544(s)	0.040	547, 598(s)	2.4×10^{-4}	505(s), 591	1.5×10^{-3}	532(s), 600	3.7×10^{-4}
7	453, 587(s)	3.7×10^{-4}	516, 541(s)	4.1×10^{-4}	497	1.3×10^{-4}	430(s), 505	5.0×10^{-4}
8	452(s), 523, 541(s)	1.3×10^{-4}	519, 547(s)	8.2×10^{-4}	452, 501(s)	1.3×10^{-3}	510	1.4×10^{-3}
9	527, 542(s)	5.9×10^{-4}	528	1.6×10^{-4}	480, 580(s)	5.2×10^{-4}	509	1.5×10^{-3}
10	542	2.1×10^{-4}	552	1.3×10^{-4}	408(s), 449, 512(s)	7.8×10^{-4}	442(s), 525, 540(s)	3.4×10^{-4}
11	402(s), 439	1.9×10^{-4}	455(s), 545	2.0×10^{-4}	406(s), 448, 509(s)	7.2×10^{-4}	440(s), 532	5.6×10^{-4}
12	434(s), 466, 508(s), 550(s)	$<10^{-5}$	434	$<10^{-5}$	405(s), 445	8.0×10^{-3}	433, 445(s)	5.6×10^{-4}
13	403, 470(s), 508, 548	$<10^{-5}$	515	$<10^{-5}$	401(s), 448	3.5×10^{-3}	400, 425(s)	$<10^{-5}$
14	420(s), 432, 450, 503(s)	4.76×10^{-5}	398, 427(s), 446	3.3×10^{-5}	403(s), 439(s), 447	9.4×10^{-4}	401, 425	4.9×10^{-5}
15	441(s), 467(s), 544	$<10^{-5}$	447	$<10^{-5}$	406, 448	2.6×10^{-3}	430	3.3×10^{-5}

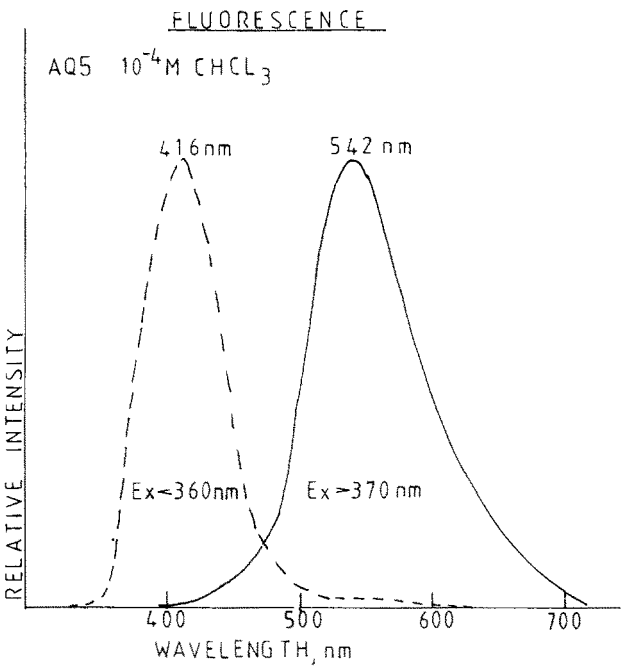

Fig. 1. Fluorescence emission spectra of 2-naphthylamidoanthraquinone in chloroform (10^{-4} M) with excitation at wavelengths greater than 370 nm (full line) and wavelengths less than 360 nm (broken line).

1–2 ms. The vibrational structure, illustrated in Fig. 2 for derivative **3**, is typical of that for anthraquinone itself [9,12] and is associated with emission from a triplet $n\pi^*$ state. Derivatives **10–15** also exhibit similar short-lived triplet emission spectra with strong $n\pi^*$ characteristics. The second group representing structures **5** and **7–9** exhibits weak phosphorescence emission with a longer triplet lifetime in the region of 5–90 ms. A typical example is illustrated in Fig. 2 for derivative **7** and is normally associated with emission from a lower lying triplet $\pi\pi^*$ state. The third group comprises derivatives **4** and **6** which exhibit both emission spectra depending on the wavelength used for excitation. This effect is illustrated in Fig. 3 for excitation wavelengths of 320 and 360 nm in ethanol as solvent. Using the longer wavelength excitation band, only a broad structureless emission spectrum was observed with a maximum at 599 nm. At shorter wavelengths, however, a very broad spectrum was observed containing what appeared to be two types of spectrum. The first was a typical structured spectrum similar to that observed for the other derivatives with $n\pi^*$ character, whereas the second was broad and structureless typical of that from a triplet state with $\pi\pi^*$ character. Because of the evident overlap in the wavelengths, the lifetimes are composite values, but they do suggest the predominance of the latter type of state. Similar excitation spectra were obtained for both emissions indicating no contribution from impurities.

4. Energy levels

All of the derivatives examined here, apart from those that exhibited anomalous behaviour in chloroform, exhibit low

Table 3
Phosphorescence data for 2-substituted anthraquinones in ethanol at 77 K

Anthraquinone	Emission wavelength (nm)	ϕ_P	τ_P (ms)
1	409(s), 457, 491, 534, 585	0.34	1.88
2	408(s), 437, 459, 494, 537, 586	0.18	1.38
3	407, 437, 459, 494, 537, 586	0.36	2.28
4	459(s), 493(s), 573, 599(br)	1.3×10^{-3}	13.26
5	524, 552(s)	0.07	13.31
6	428(s), 454(s), 492(s), 536(br), 584(br)	4.8×10^{-4}	6.81
7	531(br)	0.11	11.48
8	531(br)	0.05	90.01
9	533(br), 571(s)	2.59×10^{-3}	5.47
10	457(s), 490, 534, 586(s)	0.1	2.55
11	411(s), 437(s), 457(s), 490, 534(s), 582(s)	0.33	2.68
12	459, 495, 537, 587(s)	0.26	2.3
13	413(s), 458(s), 493, 538, 587(s)	0.16	2.36
14	409(s), 439(s), 459, 493, 537, 588(s)	0.09	2.26
15	410(s), 436(s), 456, 470(s), 490, 533, 578(s)	0.22	4.12

(s) = shoulder; (br) = broad and structureless; excitation wavelength = 290 nm; benzophenone as standard, $\phi_P = 0.74$ (ethanol); values within 96% confidence limits.

fluorescence quantum yields. The results observed may be accounted for by the effect of molecular structure on the energies of the first excited $^1\pi\pi^*$ states. For derivatives **1–3** and **10–15**, it is evident that the lowest singlet and triplet states are $n\pi^*$ in character and clearly account for the lack of fluorescence and strong structured phosphorescence spectra. Certainly, for compounds **1–3**, the lack of observable fluorescence and the high phosphorescence quantum yields may be accounted for by an internal heavy atom effect. Energy level diagrams for the remaining derivatives are illustrated in Figs. 4 and 5. The values of the respective energy levels were estimated in the following ways: (1) by assuming that the energy levels of the first $^1n\pi^*$ and $^3n\pi^*$ levels are similar to those of anthraquinone [13]; this assumption is valid in view of the relative insensitivity of the $n\pi^*$ energy levels to the extent of the π system [14]; (2) by assuming that the zeroth vibrational level of the $^1\pi\pi^*$ state corresponds to an average of the long-wavelength absorption and fluorescence maxima; (3) by taking the energies of the first excited $^3\pi\pi^*$ states from the phosphorescence emission maxima.

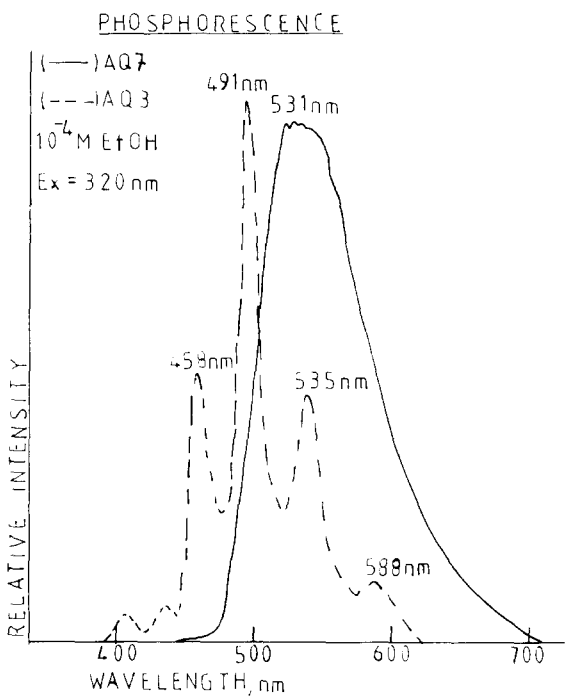

Fig. 2. Phosphorescence emission spectra of 2-(2-ethyl)hexylamidoanthraquinone (full line) and 2-(1,1,1-trichloromethyl)anthraquinone (broken line) in ethanol (10^{-4} M) with excitation at 320 nm.

Fig. 4 for derivatives **5** and **7–9** shows that the $^1n\pi^*$ and $^1\pi\pi^*$ levels are very close. Vibronic coupling between almost degenerate $^1n\pi^*$ and $^1\pi\pi^*$ levels of heteroaromatic molecules is predicted to result in pseudo- Jahn–Teller distortion of the lower state, leading to an enhanced Franck–Condon factor and consequently rapid deactivation (via either internal conversion or intersystem crossing) of the lowest excited singlet state [15]. This effect, which has been observed in studies on both aromatic carbonyl compounds [15] and nitrogen heterocycles [16], clearly explains the lack of fluorescence from the anthraquinone derivatives. Furthermore, the second excited $^3n\pi^*$ state lies just below that of the lowest excited $^1\pi\pi^*$ state enhancing the possibility of intersystem crossing due to the small size of the potential energy gap and the fact that the two states have different configurations [15]. Following relatively efficient intersystem crossing to the $^3n\pi^*$ state, further rapid deactivation occurs by internal conversion within the triplet manifold to the lowest excited $^3\pi\pi^*$ state. The latter would account for the relatively longer triplet lifetimes.

In the case of derivatives **4** and **6**, the construction of an energy level diagram in the same way shows that the $^1\pi\pi^*$ level lies below that of the second excited $^3n\pi^*$ state. Under this condition, rapid intersystem crossing between the two states would be unfavourable at low temperatures. However,

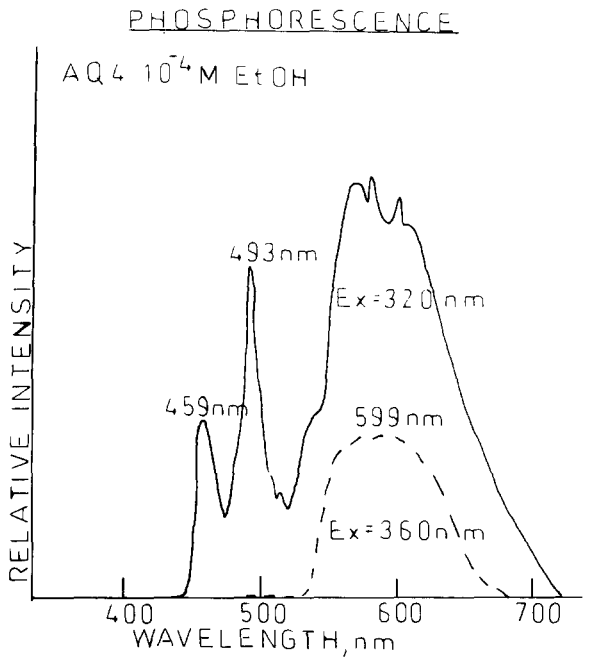

Fig. 3. Phosphorescence emission spectra of 2-(4-phenyl)thiazole-anthraquinone in ethanol (10^{-4} M) with excitation at 320 nm (full line) and 360 nm (broken line).

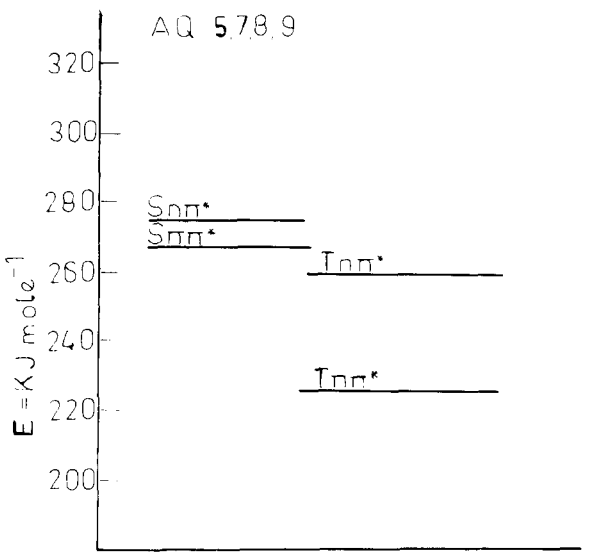

Fig. 4. Typical energy level diagram for anthraquinone derivatives **5**, **7**, **8** and **9** in ethanol.

excitation of the molecules with higher energy radiation populating the second excited $^1n\pi^*$ state would encourage intersystem crossing to the second excited $^3n\pi^*$ state, albeit weakly. The lowest excited triplet $^3\pi\pi^*$ level is lower in energy than that shown for the other derivatives in Fig. 4. This would make internal conversion less favourable and account for the observed partial structured emission shown in Fig. 3 when using higher excitation wavelengths. Partial emission from the lowest $^3\pi\pi^*$ state is observed and is consistent with the low quantum yields and long triplet lifetimes expected from a state with this configuration. This would also be equally applicable to weak intersystem crossing from the

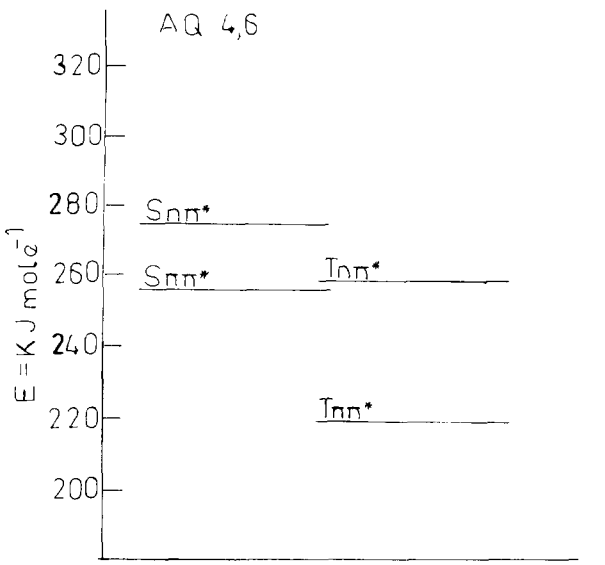

Fig. 5. Typical energy level diagram for anthraquinone derivatives **4** and **6** in ethanol.

lowest excited $^1\pi\pi^*$ state. It is noted that, with increasing dielectric strength of the solvent used (Table 2), both derivatives **4** and **6** exhibit a marked decrease in fluorescence quantum yield. This effect can be associated with a gradual increase in the energy of the lowest $^1\pi\pi^*$ state with respect to that of the $^3n\pi^*$ state giving rise to an eventual reversal similar to that exhibited in Fig. 4 for derivatives **5** and **7–9**. Rapid intersystem crossing would then account for the lack of fluorescence. In chloroform, a lowering of the energy of the $^1\pi\pi^*$ level may also account for the high fluorescence quantum yields in this solvent (rather than exciplex formation). Compound **4** is also unusual in that it may exhibit twisted intramolecular charge transfer behaviour which would certainly account for the reduced phosphorescence quantum yield.

5. Conclusions

Thus, from the spectral characteristics of these anthraquinone derivatives, it should be possible to understand and interpret the photochemical behaviour by reference to the photoinitiation activity. This is particularly important in terms of the relative energy levels when using different sources of radiation for excitation. Anthraquinones with electron-withdrawing groups and a low-lying triplet $n\pi^*$ state would be expected to be more active than those which possess electron-donating groups. However, in the presence of a tertiary amine and under polychromatic illumination, the effects are expected to be markedly different. In this case amido derivatives with long- wavelength charge transfer bands and mixed $n\pi^*/\pi\pi^*$ triplet states may tend to be more reactive. The ability of the photoinitiator to form an intermediate semiquinone radical via hydrogen atom abstraction would be an important primary mechanism, e.g. with compounds **1–3**.

Electron transfer would be more important in the presence of an amine co-synergist. The haloanthraquinones may also undergo an additional mechanism involving dehalogenation and this will be the subject of Part 2 of this series. The bromine and chlorine radicals may then participate in the overall initiation mechanism.

Acknowledgements

The authors wish to thank Zeneca Specialities for facilities for carrying out this work and EPSRC for a grant supporting G.P. Travel support from NATO, Brussels in undertaking this work is also acknowledged.

References

[1] H. Bottcher, J. Bendig, M.A. Fox, G. Hopf and H.J. Timpe, *Technical Applications of Photochemistry*, Deutscher Verlag für Grundstoffindustrie, Leipzig, 1991.
[2] N.S. Allen and J.F. McKellar, *Macromol. Rev., 13* (1978) 241.
[3] J.F. McKellar and N.S. Allen, *Photochemistry of Man-Made Polymers*, Applied Science Publishers, London, 1979.
[4] N.S. Allen and J.F. McKellar, in N.S. Allen (ed.), *Developments in Polymer Photochemistry*, Vol. 1, Applied Science Publishers, London, 1980, Chapter 7, p. 191.
[5] N.S. Allen and J.F. McKellar, *Photochemistry of Dyed and Pigmented Polymers*, Applied Science Publishers, London, 1980.
[6] N.S. Allen, J.P. Hurley, D. Bannister and G.W. Follows, *Eur. Polym. J., 28* (1992) 1309.
[7] N.S. Allen, J.P. Hurley, D. Bannister, G.W. Follows, S. Navaratnam and B.J. Parsons, *J. Photochem. Photobiol. A: Chem., 68* (1992) 213.
[8] N.S. Allen, J.P. Hurley, A. Rahman, G.W. Follows and I. Weddell, *Eur. Polym. J., 29* (1993) 1155.
[9] N.S. Allen, J.P. Hurley, M. Edge, G. Follows, I. Weddell and F. Catalina, *J. Photochem. Photobiol. A: Chem., 71* (1993) 109.
[10] J.N. Demas and G.A. Crosby, *J. Phys. Chem., 75* (1971) 991.
[11] N.S. Allen, F. Catalina, C. Peinado, R. Sastre, J.L. Mateo and P.N. Green, *Eur. Polym. J., 23* (1987) 985.
[12] J.G. Calvert and J.N. Pitts, *Photochemistry*, Wiley, New York, 1966.
[13] N.S. Allen, P. Bentley and J.F. McKellar, *J. Photochem., 5* (1976) 225.
[14] V.G. Plotnikov, *Opt. Spectrosc. (USSR), 20* (1966) 589.
[15] R.M. Hochstrasser and C.A. Marzzacco, in E.C. Lim (ed.), *Int. Conf. on Molecular Luminescence*, Benjamin, New York, 1969, p. 631.
[16] R. Li and E.C. Lim, *J. Chem. Phys., 57* (1972) 605.